Yang *et al. Geoscience Letters* (2023) 10:32
https://doi.org/10.1186/s40562-023-00288-5

Geoscience Letters

RESEARCH LETTER

Open Access

Uncertainties of monthly ocean bottom pressure from Gravity Recovery and Climate Experiment (GRACE): a case study at the Drake Passage

Chengcheng Yang[1,2], Xuhua Cheng[1,2*] and Jianhuang Qin[1,2]

Abstract

Several studies reported some aliasing errors of Ocean bottom pressure (OBP) data from Gravity Recovery and Climate Experiment (GRACE), although this data have been widely used to estimate the oceanic transports. In this study, the performances of monthly OBP data from six GRACE products with two different solutions are evaluated by comparisons with the observed records at the Drake Passage. Result shows that spherical harmonic products have a better ability to capture monthly OBP variability than mascon products at the Drake Passage. In all GRACE products, higher skills occur to the south of Polar Front than those in the northern Drake Passage, and the correlations with observations reach minimum in the Local Dynamics Array (LDA) region. Such spatial differences are mainly attributed to local mesoscale processes, accompanied with high-frequency bottom eddy kinetic energy (EKE). It indicates that the monthly OBP variations from GRACE products are not reliable in the eddy-rich regions.

Keywords Ocean bottom pressure, GRACE, Drake Passage, Eddy kinetic energy

Introduction

The low-frequency variations of ocean bottom pressure (OBP), which are primarily associated with fluctuations in ocean mass, has been used in the studies of sea level changes and large-scale transports (Cheng and Qi 2010; Hughes et al. 1999). Thanks to the launch of the Gravity Recovery and Climate Experiment (GRACE) mission (Tapley et al. 2004), a unique way is provided to obtain global OBP data, which has greatly advanced the understanding of oceanic dynamics, such as the global mean sea level budget (Chambers et al. 2017; Leuliette and Miller 2009) and regional sea level change (Kleinherenbrink et al. 2016; Qin et al. 2022; Wang et al. 2015). In addition, satellite-based OBP data perform well in monitoring the basin-wide oceanic transports on seasonal to interannual variations (Liau and Chao 2017; Makowski et al. 2015; Mazloff and Boening 2016), even the deep ocean transport variability through the Luzon Strait (Zhu et al. 2022). Thus, the GRACE OBP data have already played an unprecedented role in oceanic transport, and a long-term sustained monitor of the ocean transports seems achievable based on GRACE products.

However, the monthly OBP data from GRACE products remain some aliasing errors. Previous studies shown non-negligible discrepancies of OBP estimations among different GRACE products obtained with different processing solutions (Blazquez et al. 2018; Chambers and Bonin 2012). Besides, the aliasing errors of GRACE products also arose from their inabilities to distinguish the high-frequency signals with the periods less than 60 days (Quinn and Ponte 2011). All these issues lead to

*Correspondence:
Xuhua Cheng
xuhuacheng@hhu.edu.cn
[1] Key Laboratory of Marine Hazards Forecasting, Ministry of Natural Resources, Hohai University, No. 1 Xikang Road, Nanjing 210098, China
[2] College of Oceanography, Hohai University, Nanjing, China

© The Author(s) 2023. **Open Access** This article is licensed under a Creative Commons Attribution 4.0 International License, which permits use, sharing, adaptation, distribution and reproduction in any medium or format, as long as you give appropriate credit to the original author(s) and the source, provide a link to the Creative Commons licence, and indicate if changes were made. The images or other third party material in this article are included in the article's Creative Commons licence, unless indicated otherwise in a credit line to the material. If material is not included in the article's Creative Commons licence and your intended use is not permitted by statutory regulation or exceeds the permitted use, you will need to obtain permission directly from the copyright holder. To view a copy of this licence, visit http://creativecommons.org/licenses/by/4.0/.

uncertainties of the estimations of OBP trend and high-frequency variability in the ocean transports (Makowski et al. 2015; Mazloff and Boening 2016). By comparing with in-situ OBP records, recent studies also revealed that the accuracy in GRACE products shows large spatial difference in the Kuroshio Extension and South China Sea (Park et al. 2008; Wang et al. 2023). However, the verifications between the GRACE products and in-situ observations are always sporadic in the Southern Ocean due to the paucity of bottom pressure recorders. Given the active mesoscale activities in the Southern Ocean (Rintoul and Sokolov 2001; Sokolov and Rintoul 2007), the selection of in-situ locations may have a large impact on the verifications of GRACE products. All these things should be understood more clearly.

The Antarctic Circumpolar Current (ACC) plays a vital role in regulating climate system and the carbon cycle (Meredith et al. 2011; Rintoul 2018), but its researches are still extremely limited compared with other strong currents. The Drake Passage, as the narrowest constriction of the ACC, has relative more in-situ observations (Meredith et al. 2011). In particular, bottom pressure recorders were deployed at the Drake Passage since 1979 (Gille 1999; Hughes et al. 1999; Whitworth et al. 1982), and OBP data from these sites were used to calculate the variation of ACC transports (Meredith et al. 2004). In recent years, there are many long-term sustained monitoring programs conducting in the Drake Passage, such as the cDrake experiment (Donohue et al. 2016). The cDrake experiment contains 46 Current and Pressure-recording Inverted Echo Sounders (CPIES) sites moored across the Drake Passage from November 2007 to November 2011 (Chereskin et al. 2012), continuously providing hourly observed OBP and near-bottom current velocities. Based on CPIES measurements, previous studies have examined the mean transport and the vorticity balance at the Drake Passage (Donohue et al. 2016; Firing et al. 2016). Hence, the in-situ OBP records can be used to evaluate and improve the quality of GRACE products.

In this paper, we evaluate the performance of six GRACE products by comparisons with in-situ OBP records from CPIES sites at the Drake Passage. The remainder of this paper is organized as follows. Data and methods are presented in section "Data and methods". In section "Results", the assessments of six GRACE products are investigated. Conclusions and discussion are given in section "Conclusions and discussion".

Data and methods

In this study, monthly OBP data from six GRACE products are used. Three of them are based on spherical harmonic solutions from Center for Space Research (CSR), Jet Propulsion Laboratory (JPL), and GeoForschungsZentrum Potsdam (GFZ), named as CSR RL06.3, JPL RL06.3 and GFZ RL06.3 products, respectively. The other three products are based on mascon solutions (separating the Earth into equal-area mass concentration cells) from CSR (with an area equivalent to 1°×1° at the equator), JPL (with an area equivalent to 3°×3° at the equator), and NASA Goddard Space Flight Center (GSFC, with an area equivalent to 1°×1° at the equator), named as CSR RL06.2 M, JPL RL06.2 M and GSFC RL06.2 M products, respectively. In this study, the above six GRACE products are referred to as CSR–HR, JPL–HR, GFZ–HR, CSR–MAS, JPL–MAS and GSFC–MAS, respectively. The CSR–HR, JPL–HR and GFZ–HR have same spatial grid points with the horizontal resolution of 1°×1° (Chambers and Willis 2010). The horizontal resolution of JPL–MAS and GSFC–MAS is 0.5°×0.5°, while the resolution is 0.25°×0.25° for CSR–MAS (the grid point locations of six GRACE products are shown in Additional file 1: Fig. S1).

In-situ de-drift OBP records and near-bottom currents are obtained from the cDrake experiment. As shown in Fig. 1a, 46 CPIES sites cover one meridional (black triangles, C line Array) and three zonal lines [red triangles, Local Dynamics Array (LDA)]. There are also five CPIESs across the Shackleton Fracture Zone (SFZ; magenta triangles, H array). More detailed information of CPIES records is listed in Additional file 1: Table S1. When calculating monthly data by CPIES records, the hourly records are first averaged into daily mean, but the daily data are set as missing values if hourly data account for less than half of the day (Additional file 1: Fig. S1c). Then, a 30-day low-pass Butterworth filter was applied on the daily data to eliminate influence of extreme values within month on the monthly mean results. The CPIES records span from November 2007 to November 2011. The OBP anomalies from both satellite and in-situ data are converted to equivalent water heights (cm) using a constant reference density of 1025 kg/m^3 and the gravitational acceleration 9.8 m/s^2. Student's *t* test on the basis of a difference between sample means is used to test the statistical significance of the correlation coefficient.

The daily absolute dynamic topography (ADT) data are obtained from Archiving Validation and Interpretation of Satellite Data in Oceanography (AVISO) with a 0.25°×0.25° horizontal resolution. Daily OBP data from dynamically consistent ocean state estimate, Estimating the Circulation and Climate of the Ocean Version 4, Release 4 (ECCO V4r4) and eddy-permitting model-Estimating the Circulation and Climate of the Ocean-Phase II (ECCO2) are also used in this study, with a horizontal resolution of 0.5°×0.5° and 0.25°×0.25°, respectively.

The correlation, root-mean-square errors (RMSE) and average amplitude errors (ERR_{amp}, which provides a

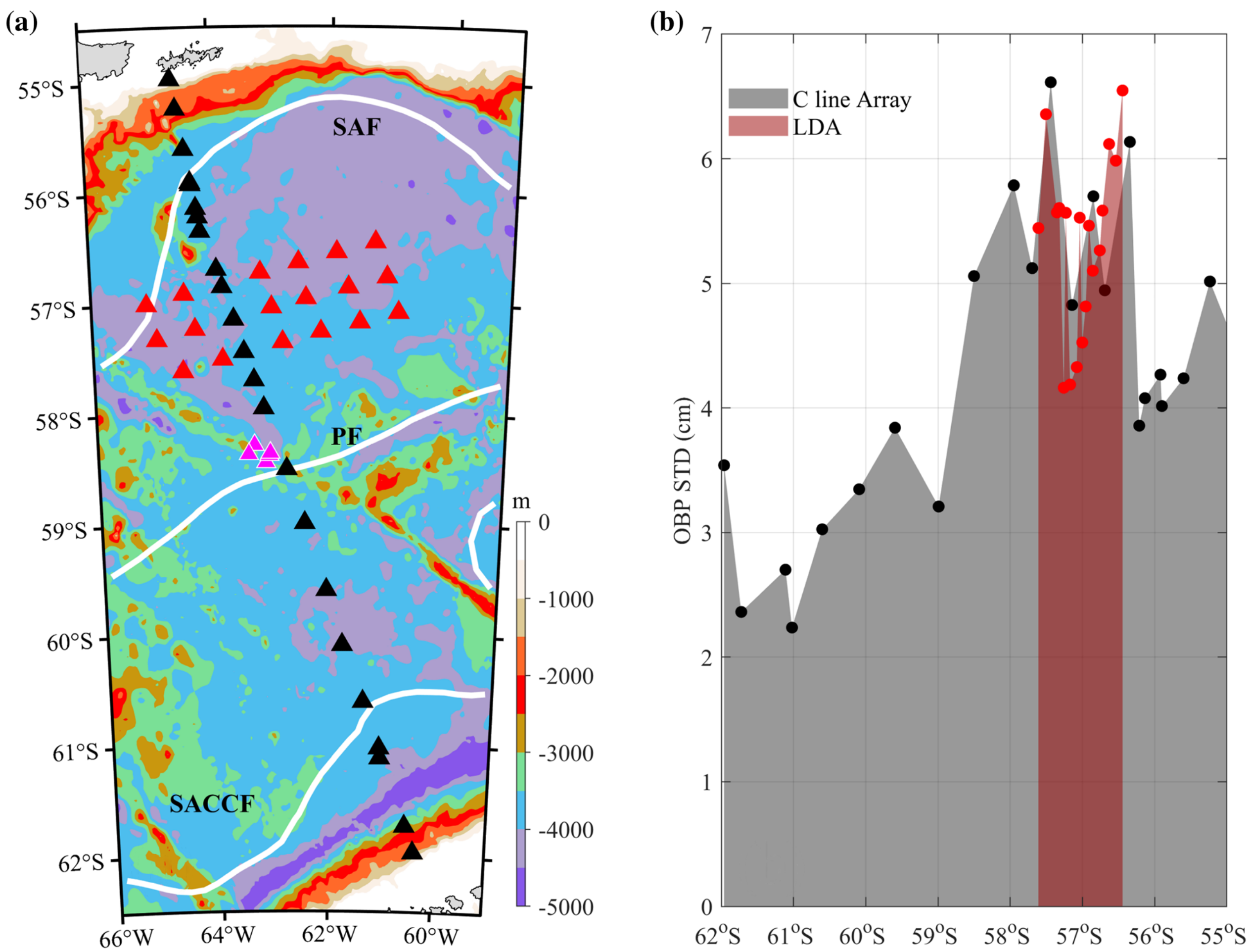

Fig. 1 **a** Spatial distributions of 46 CPIES at the Drake Passage. The C line Array and Local Dynamics Array (including A, B, D, E, F and G arrays) are labelled by black and red triangles, respectively, while H arrays are shown with magenta triangles. White lines denotes the Subantractic Front (SAF), Polar Front (PF) and Southern ACC Front (SACCF). **b** Standard deviations of in-situ OBP vs latitude and color-coded by location from C line Array (grey shading and dots) and LDA (red shading and dots) reocrds

measure of the average difference between the two time series, $\mathrm{ERR}_{\mathrm{amp}} = \frac{1}{N}\sum_{t=1}^{N}|\mathrm{OBP}_{\mathrm{GRACE}}(t) - \mathrm{OBP}_{\mathrm{PIES}}(t)|$, see Rashid et al. 2010) are used to assess the quality of monthly OBP from GRACE products. Prior to comparing the OBP variabilities between satellite and in-situ data, all GRACE data were interpolated onto the CPIES site locations using 2-D linear interpolation. The choice of interpolation method, such as nearest interpolation, does not have an impact on the extraction of grid data from different horizontal resolution products in this study (not shown).

Results

OBP variations at the Drake Passage

There are three common oceanic fronts over the Drake Passage, i.e., Subantractic Front (SAF), Polar Front (PF) and Southern ACC Front. Following Kim and Orsi (2014), the climatology fronts are shown in Fig. 1a with white contours. The standard deviations (STD) of OBP is around 5 cm to the north of PF, and is below 4 cm in the southern Drake Passage. To minimize the influence of spatial non-uniformity in CPIES, we focused on the C line Array (black triangles in Fig. 1a) when calculating the averaged OBP variation at the Drake Passage. Figure 2a presents the variations of OBP anomalies derived from in-situ records (black lines), as well as those from CSR–HR, JPL–HR, and GFZ–HR (green, red, and blue lines, respectively). Similarly, Fig. 2b illustrates the variations of OBP derived from CSR–MAS, JPL–MAS, and GSFC–MAS (green, red, and blue lines, respectively). One can see that both in-situ and GRACE data exhibit troughs in May 2011, while there are no significant peaks in August 2009 from CSR–HR, JPL–HR and GFZ–HR. Nevertheless, the OBP variabilities from GRACE products using

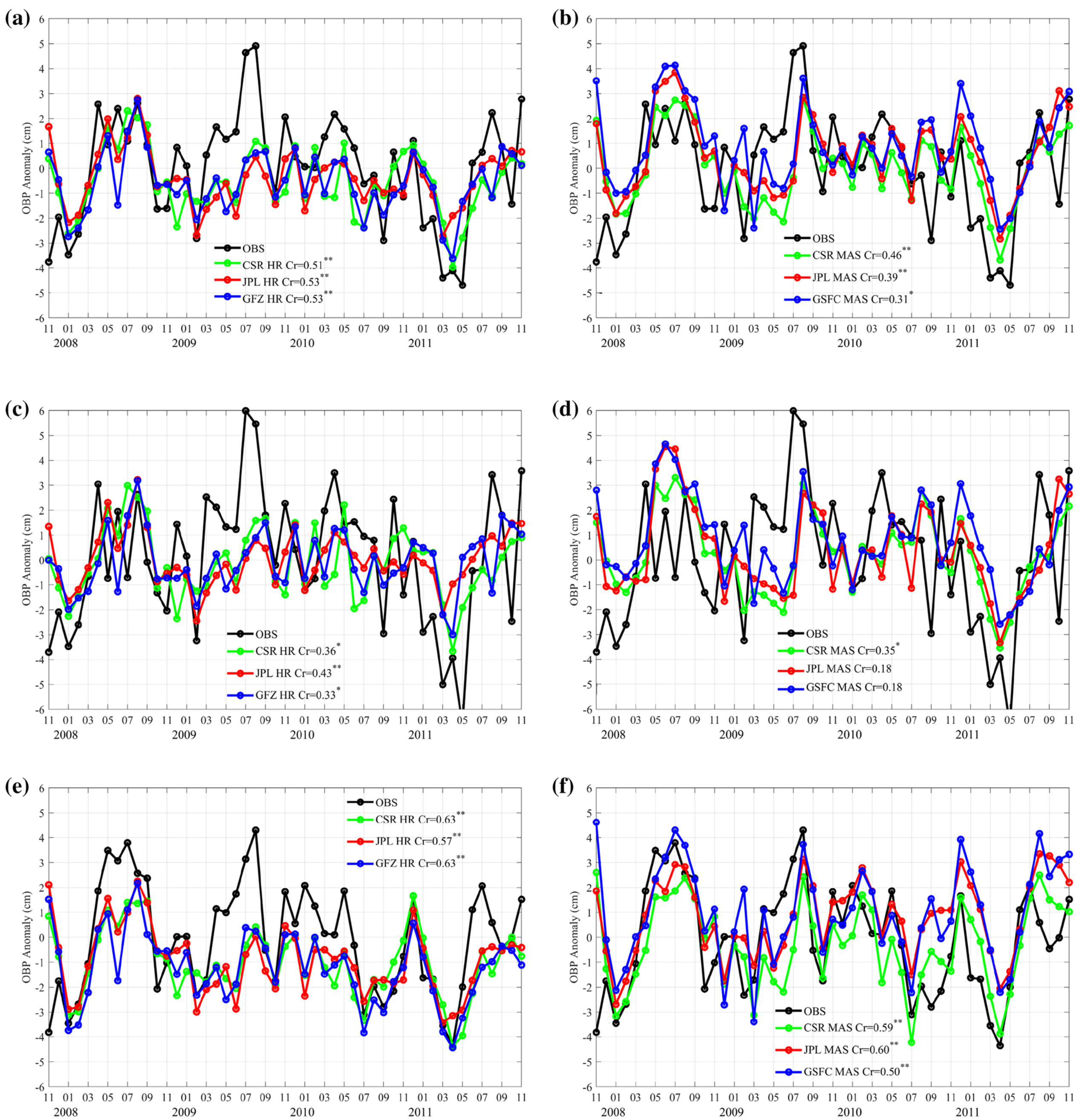

Fig. 2 Monthly OBP time series from in-situ records (black lines) and GRACE products (color lines) averaged in the C line Array. The left panels are for the HR products, and the right panels are for the mascon products; the upper, middle, and lower panels are for the whole array, the northern part and the southern part, respectively. The superscript * (**) indicates the correlation coefficient is above the 95% (99%) confidence level, 0.29 (0.37)

spherical harmonics solutions (i.e., CSR–HR, JPL–HR and GFZ–HR) have considerable variabilities during the study period (color lines). All of them have high correlation coefficients with the in-situ OBP records (higher than 0.5), significant at the 99% confidence level (Cr = 0.37). In contrast, although CSR–MAS, JPL–MAS and GSFC–MAS have been proved to perform better in land signal leakage, especially in polar regions (Chambers & Bonin 2012; Watkins et al. 2015), their correlation coefficients with in-situ OBP records are relatively lower at the Drake Passage (Fig. 2b; Cr = 0.46, 0.39, and 0.31, respectively). Moreover, both RMSE and ERR_{amp}

of spherical harmonic products are lower than those of mascon products (Table 1), which is consistent with the correlation results.

Spatial difference in the accuracy of GRACE OBP

Due to the spatial difference of OBP STD (Fig. 1b), the C line Array is divided into the northern and southern regions based on the PF. Figure 2c, and d shows the monthly OBP averaged in the northern region. As shown in Fig. 2c, the OBP time series from CSR–HR, JPL–HR and GFZ–HR all have significant correlations with in-situ OBP time series (Cr = 0.36, 0.43, 0.33, respectively), significant at the 95% confidence level (Cr = 0.29). However, correlation coefficients are insignificant between CPIES records and GRACE products using mascon solutions, except for CSR–MAS (Fig. 2d). In the southern region (Fig. 2e, and f), the OBP time series from all GRACE products have significant correlations with CPIES records (over 0.50), significant at the 99% confidence level (Cr = 0.37). The spherical harmonics solutions still show relative high correlation coefficients both in the northern and southern Drake Passage, with RMSE and ERR_{amp} lower than mascon solutions (Table 1).

To better understand the north–south difference of the accuracy of GRACE OBP products, we also calculated the pointwise correlation coefficients of CPIES records with six GRACE products at the Drake Passage. As shown in Fig. 3, the spatial distributions of correlation coefficients are quite different between spherical harmonics products and mascon products. The numbers of sites with correlation coefficients significant at the 95% confidence level (filled circles) are 26, 30 and 23 in CSR–HR, JPL–HR and GFZ–HR (Fig. 3a–c). In contrast, the numbers of significant correlation coefficients are 26, 22 and 13 in CSR–MAS, JPL–MAS and GSFC–MAS (Fig. 3d–f). Combining the results in Figs. 2 and 3, we can surmise that spherical harmonics solutions perform better than mascon solutions in capturing the monthly OBP variability in the Drake Passage. In addition, the main differences among them are concentrated in the northern region. One can see that the correlation coefficients in the southern region are higher than those in the northern region in all GRACE products. The correlation coefficients are lowest in north meandering branch and the western and northeastern parts of LDA region (the downstream of the ACC crossing the SFZ topography).

Influence of local mesoscale process

To further explore the possible reason for poor performance in the such regions, the characteristic length scale of monthly OBP variability is calculated at each site using CPIES records. At each site (effective record length longer than 24 months), the spatial correlation coefficients between it and the other OBP time series are fitted to a Gaussian curve using the least squares method (Park et al. 2008), which is calculated as follows: $G(r) = e^{-(r/r_0)^2}$ (where r is the horizontal distance with other sites). The characteristic length scale r_o is the distance when the Gaussian curve reach e^{-1} at each site. As shown in Fig. 4a, the characteristic length is larger in the southern passage and smaller in the northern passage, especially in the LDA region. To better understand whether the characteristic length is related to the uneven north–south distribution of CPIES sites, the Gaussian curves were computed using all CPIES records and only C line Array records. Here, the results at sites C8 and C14 (represented by dots with magenta edges in Fig. 4a) are presented in Fig. 4b, and d, and Fig. 4c, and e, respectively. It can be seen that the uneven distribution of CPIES sites does not significantly affect the shape of the Gaussian curve. In addition, uncertainties of r_o were calculated for each site, and they were found to be considerably smaller than the r_o values (see Additional file 1: Table S2). In general, the small (large) characteristic length scales are always coincided with eddy rich (poor) regions (Park et al. 2008). It can be verified from the spatial pattern of bottom EKE (30–150-day bandpass filtered velocity anomalies) from in-situ records (Fig. 5a). The filter is applied due to the power spectrum of daily OBP and bottom velocity at the Drake Passage, which show energetic intra-seasonal variability (Additional file 1: Fig. S2). In addition, the spatial distribution of the surface EKE was also computed using AVISO absolute geostrophic velocities with 30–150-day bandpass filter

Table 1 Root-mean-square errors (RMSE) and average amplitude errors (ERR_{amp}) between CPIES records and GRACE products

		CSR–HR	JPL–HR	GFZ–HR	CSR–MAS	JPL–MAS	GSFC–MAS
All	RMSE (cm)	1.97	1.98	2.04	2.01	2.20	2.45
	ERR_{amp} (cm)	1.54	1.49	1.54	1.59	1.76	1.95
North	RMSE (cm)	2.52	2.38	2.51	2.55	2.91	2.95
	ERR_{amp} (cm)	2.01	1.93	2.01	2.06	2.37	2.45
South	RMSE (cm)	1.94	1.90	1.94	1.88	1.98	2.32
	ERR_{amp} (cm)	1.52	1.44	1.52	1.48	1.60	1.77

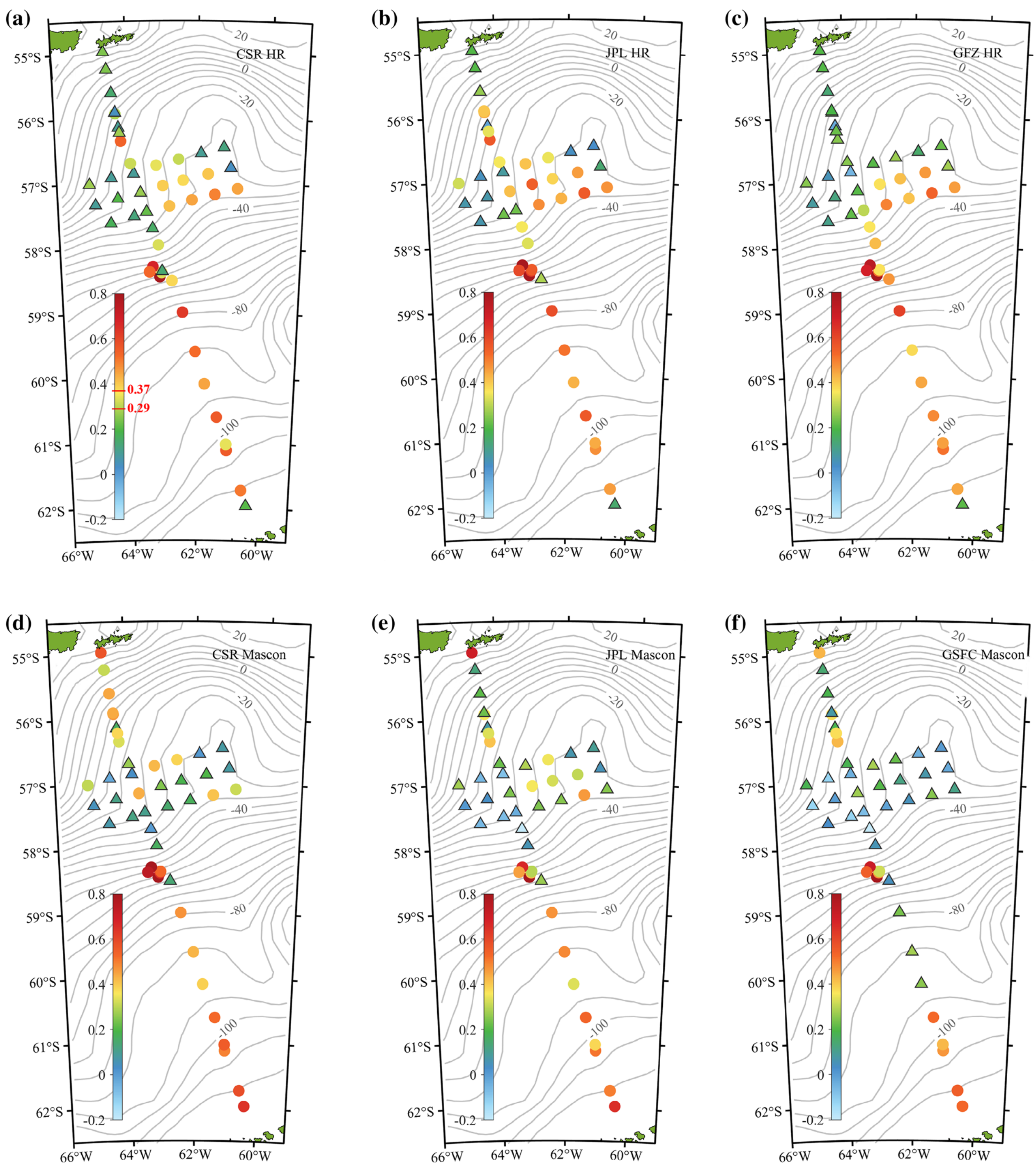

Fig. 3 Pointwise correlations between the CPIES records and GRACE products. Results non-significant at the 95% confidence level are represented with triangles. The mean absolute dynamic topography from AVISO between November 2017 and November 2011 is shown with grey contours, with contour intervals of 5 cm

(Fig. 5b). The result reveals that EKE is stronger in the LDA region and weaker in the southern passage, both at the surface and bottom. Notably, there are significant correlations between the EKE calculated from AVISO data and that from CPIES records in the high EKE region (Additional file 1: Fig. S3). These results are consistent with Chereskin et al. (2009), that the eddies coinciding with meanders in the surface fronts is consistent with

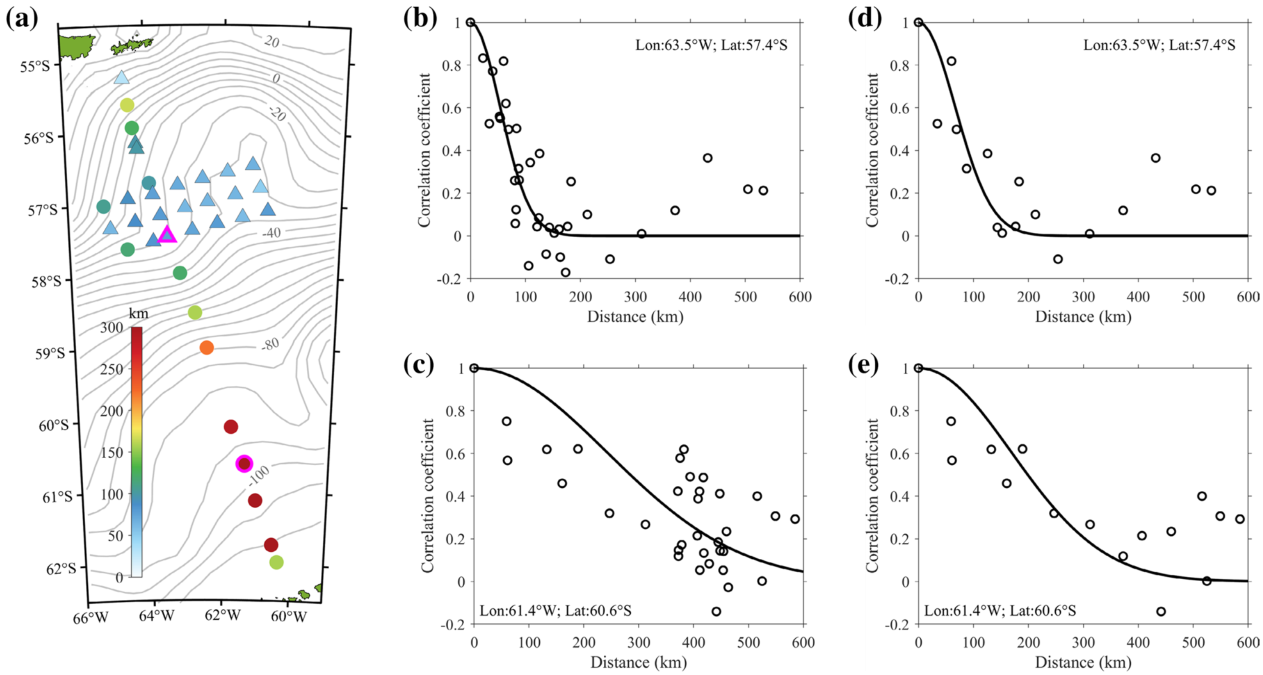

Fig. 4 **a** Spatial distribution of characteristic length scale. The definition of characteristic length scale is shown in section "Results". Triangles indicate the characteristic lengthes less than 100 km. Dots with magenta edges are selected to show the fitted curve. The mean absolute dynamic topography from AVISO between November 2017 and November 2011 is shown with grey contours, with contour intervals of 5 cm. **b**, **c** Spatial correlations at sites C8 and C14 superimposed by Gaussian fitted curves computed using all CPIES OBP records. **d**, **e** Are same as **b** and **c** but using only OBP records in C line Array

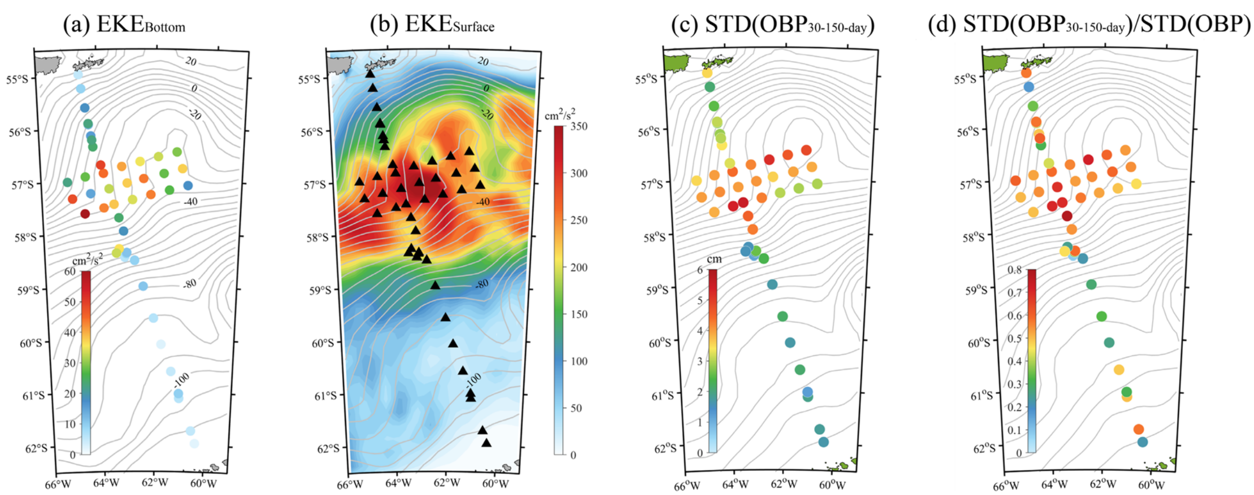

Fig. 5 **a** Distribution of bottom EKE from CPIES near-bottom current. **b** Distribution of surface EKE from AVISO surface current. **c** Standard deviations of 30–150-day bandpass filtered in-situ OBP at each site. **d** Ratios between the result in (c) and the total standard deviations of in-situ OBP time series

deep eddies. Such occurrence of mesoscale processes, accompanied oscillations of water mass, is very likely to favor the intra-seasonal variability of OBP (Fig. 5c). As a result, the 30–150-day OBP signals can explain approximately 60% of total OBP variances in the LDA region (Fig. 5d). It is also suggested by an additional power spectrum analysis of in-situ OBP that the signals of OBP are active at 30–150 days in the northern passage (red line in Additional file 1: Fig. S4a), but much weaker in the southern passage (blue line in Additional file 1: Fig. S4a). Thus, it is reasonably deduced that the local mesoscale processes are the key factor for the spatial difference in the accuracy of GRACE products in the Drake Passage.

Previous studies have reported that meandering of the ACC is always pronounced in the lee of topography (Thompson and Sallee 2012), leading to high EKE downstream of the topography (Dufour et al. 2015). In the case of the Drake Passage, it can be seen in Fig. 5a, b that mesoscale signals are relatively active in northern region, and EKE decreases rapidly to the south of the PF. The scatter plots of bottom EKE and correlation coefficients between GRACE products and CIPES records are shown in Fig. 6. Regression lines reveal the significant negative relationship between the performance of GRACE products and bottom eddy activities with the independence of different solutions used in GRACE products. The scatter plots of surface EKE and correlation coefficients between GRACE products and CIPES records were also computed, which are similar to those in Fig. 6 (see Additional file 1: Fig. S5). Moreover, it is worth noting that the mascon products exhibit slightly higher regression coefficients compared to the spherical harmonic products, which can be attributed to their poorer performance in high EKE regions, as shown in Figs. 2 and 6. Mascon products primarily rely on the OBP variations in fixed spatial regions and do not undergo spatial Gaussian smoothing, unlike spherical harmonic products. Considering that GRACE data have a temporal resolution of approximately 28 days, relying heavily on signals predominantly driven by intra-seasonal variations (see Fig. 5d) can introduce additional errors in OBP when estimating monthly signals in mascon products. In this study, the correlation coefficient of 0.29 is the threshold for the accuracy of GRACE products at the 95% confidence level. The regression lines surpass the threshold only when the bottom EKE is below 28.2, 29.4, 27.6, 22.8, 18.2 and 7.9 cm^2/s^2 for CSR–HR, JPL–HR, GFZ–HR, CSR–MAS, JPL–MAS and GSFC–MAS, respectively. Therefore, we can surmise that GRACE products cannot resolve the OBP variability quite well in the area with high EKE. The relatively poor performance of GRACE OBP in high EKE regions can be attributed to both the horizontal resolution and sampling frequency of the GRACE satellites. The original horizontal resolutions of all six GRACE products exceed 100 km, which hampers their ability to accurately capture the local OBP variability when the characteristic length scale is smaller than 100 km (Fig. 4a). Besides, the sampling frequency of GRACE satellites is approximately 28 days, introducing errors when estimating the monthly mean value of OBP from intra-seasonal variations at a specific time (Fig. 5c, d) in high EKE regions.

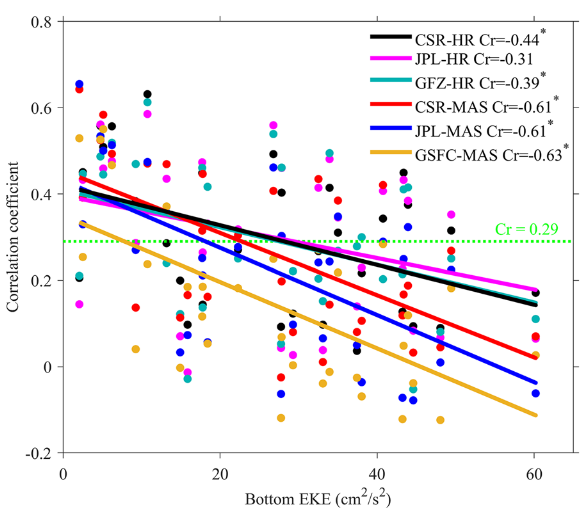

Fig. 6 Scatter plot of bottom EKE and correlation coefficients between CPIES records and GRACE products at each site. Black, magenta, green, orange, blue, and yellow dots (regression lines) represent the results using CSR–HR, JPL–HR, GFZ–HR, CSR–MAS, JPL–MAS, and GSFC–MAS, respectively. * indicates the 95% confidence level (0.29)

Conclusions and discussion

In this study, six GRACE products with two solutions have been evaluated by comparisons with in-situ CPIES records at the Drake Passage. Our results reveal that while the GRACE mascon products have higher spatial resolutions compared to the spherical harmonic products, the latter shows superior performance in estimating the variation of OBP averaged in the Drake Passage. Moreover, the accuracy of OBP variations have discernible spatial difference at the Drake Passage in all GRACE products, with better (worse) performance to the south (north) of PF. The correlation coefficient reaches its minimum in the LDA region and fails to pass 95% significance level. The spatial difference can be attributed to spatial distributions of bottom (or surface) EKE in the Drake Passage, which show significantly negative correlations with the performance of all GRACE products. In general, the meandering of SAF and PF promotes the occurrence of mesoscale eddies in the northern passage, accompanied with deep mesoscale eddies. This dynamic environment leads to shorter characteristic length scales of OBP variability and the active intra-seasonal variability of OBP in the northern passage. Consequently, the limitations of the GRACE satellites, such as their low-resolution (> 100 km) and low-frequency (28 days), hinder their ability to accurately capture the local OBP variability in this high bottom (or surface) EKE region.

In the context of the climatic change, variations of deep ocean circulations are important to regulate the global warming, carbon cycle and so on. OBP is expected to monitor the change of these circulations by geostrophic balance (Koelling et al. 2020; Mazloff and Boening 2016). For example, using in-situ OBP records, Chereskin et al. (2009) observed deep mesoscale eddies at the Drake Passage. Our study sheds light on the potential limitations of accurately capturing OBP signals in GRACE products, particularly in regions with high bottom (surface) EKE. Mesoscale eddies are widespread in the global oceans and contribute to more than 80% of the total ocean kinetic energy (Chelton et al. 2011; Fu et al. 2010). Therefore, assessing the performance of these products in such regions is necessary to ensure reliable measurements in the future.

Ocean models have made significant achievements in simulating time-mean ACC transport (Xu et al. 2020), however, accurately capturing the intra-seasonal signals of OBP remains a challenge in well-known models. For instance, both ECCO V4r4 and ECCO2 fail to reproduce the significant north–south differences in intra-seasonal OBP signals at the Drake Passage (Additional file 1: Fig. S4). This discrepancy may be attributed to aliasing errors introduced by the assimilation of monthly GRACE products into models. The possible ways to accurately monitor the deep ocean transports in the future may rely on the more in-situ OBP observations, improvements of OBP assimilation in ocean models, and the development of ocean models based on the mass conservation framework.

Supplementary Information

The online version contains supplementary material available at https://doi.org/10.1186/s40562-023-00288-5.

Additional file 1. Spectra analysis based on fast Fourier transform method. **Figure S1**. Spatial and temporal coverage of in-situ and GRACE data. (a) Spatial locations of 46 CPIES from cDrake experiment. Black triangles: C line; white triangles: Local Dynamics Array (including A, B, D, E, F and G arrays); magenta triangles: H array. (b) GRACE grid point positions. Red dots: spherical harmonics products from CSR, JPL and GFZ; green dots: JPL and GSFC mascon product; black dots: CSR mascon product. (c) Daily-mean ocean bottom pressure records from 46 CPIES. The x-axis represents the day number, while the y-axis represents the different stations, labeled as A1, A2, A3, B1, B2, B3, and so on. Black shaded areas indicate missing values.**Figure S2**. Variance-preserved power spectra as a function of period. (a) OBP and (b&c) bottom current velocities in the LDA region. Red lines denote 95% confidence levels.**Figure S3**. Correlation coefficients between eddy kinetic energy (EKE) calculated from AVISO geostrophic current and that from CPIES near-bottom current at each site. Results non-significant at the 95% confidence level (Cr=0.29) are represented with triangles. The mean absolute dynamic topography from AVISO between November 2017 and November 2011 is shown with grey contours, with contour intervals of 5 cm.**Figure S4**. Variance-preserved power spectra as a function of period of OBP at the Drake Passage. Black, red and blue lines represent the results averaged in the whole passage, to the north of Polar Front, and to the south of Polar Front, respectively. (a) is calculated by using in-situ observations, (b) and (c) are calculated from ECCO and ECCO2, respectively.**Figure S5**. Scatter plot of surface eddy kinetic energy (EKE) from AVISO geostrophic current and correlation coefficients between CPIES records and GRACE products at each site. Black, magenta, green, orange, blue, and yellow dots (regression lines) represent the results using CSR-HR, JPL-HR, GFZ-HR, CSR-MAS, JPL-MAS, and GSFC-MAS, respectively. * indicates the 95% confidence level (0.29).**Table S1**. The 46 CPIES records used in our study with site designators, locations and Time period.**Table S2**. The characteristic length r0 and uncertainty of r0at each site (effective value length longer than 24 months).

Acknowledgements
We want to thank two anonymous reviewers for constructive suggestions and comments.

Author contributions
XC provided financial support for this study. CY carried out data analyses, and prepared for the manuscript. JQ and XC commented on earlier versions of the manuscript. All authors read and approved the final manuscript.

Funding
Xuhua Cheng is supported by the Natural Science Foundation of China (Grant 41876002). Chengcheng Yang is supported by a scholarship from the China Scholarship Council (Grant CSC 202206710084), and Postgraduate Research and Practice Innovation Program of Jiangsu Province (Grant KYCX22_0585). Jianhuang Qin is supported by the National Natural Science Foundation of China (Grant 42106003).

Availability of data and materials
The GRACE data are downloaded from the GRACE Tellus Web site (https://podaac.jpl.nasa.gov). In-situ bottom pressure records of cDrake experiment are obtained from the University of Rhode Island Web site (https://www.po.gso.uri.edu/cdrake/data.html#cpies). Absolute dynamic topography and surface geostrophic current data are available from the Copernicus Marine Environment Monitoring Service Web site (https://doi.org/10.48670/moi-00148). WOA18 temperature and salinity fields are obtained from the NOAA National Centers for Environmental Information Web site (https://www.ncei.noaa.gov/data/oceans/woa/WOA18/DATA/). The ECCO V4r4 OBP data are available on the website https://data.nas.nasa.gov/ecco/data.php?dir=/eccodata/llc_90/ECCOv4/Release4/interp_daily/OBPNOPAB. The ECCO2 OBP data are obtained from the Asian Pacific data research center at the University of Hawaii (http://apdrc.soest.hawaii.edu/las/v6/constrain?var=4825).

Declarations

Competing interests
The authors declare that they have no competing interests.

Received: 8 May 2023 Accepted: 13 July 2023
Published online: 25 July 2023

References
Blazquez A, Meyssignac B, Lemoine JM, Berthier E, Ribes A, Cazenave A (2018) Exploring the uncertainty in GRACE estimates of the mass redistributions at the Earth surface: implications for the global water and sea level budgets. Geophys J Int 215(1):415–430. https://doi.org/10.1093/gji/ggy293
Chambers DP, Bonin JA (2012) Evaluation of Release-05 GRACE time-variable gravity coefficients over the ocean. Ocean Sci 8(5):859–868. https://doi.org/10.5194/os-8-859-2012
Chambers DP, Willis JK (2010) A Global evaluation of ocean bottom pressure from GRACE, OMCT, and steric-corrected altimetry. J Atmos Oceanic Tech 27(8):1395–1402. https://doi.org/10.1175/2010jtecho738.1
Chambers DP, Cazenave A, Champollion N, Dieng H, Llovel W, Forsberg R et al (2017) Evaluation of the global mean sea level budget between 1993 and 2014. Surv Geophys 38(1):309–327. https://doi.org/10.1007/s10712-016-9381-3
Chelton DB, Schlax MG, Samelson RM (2011) Global observations of nonlinear mesoscale eddies. Prog Oceanogr 91(2):167–216. https://doi.org/10.1016/j.pocean.2011.01.002

Cheng XH, Qi YQ (2010) On steric and mass-induced contributions to the annual sea-level variations in the South China Sea. Glob Planet Change 72(3):227–233. https://doi.org/10.1016/j.gloplacha.2010.05.002
Chereskin TK, Donohue KA, Watts DR, Tracey KL, Firing YL, Cutting AL (2009) Strong bottom currents and cyclogenesis in Drake Passage. Geophys Res Lett. https://doi.org/10.1029/2009gl040940
Chereskin TK, Donohue KA, Watts R (2012) cDrake: dynamics and transport of the antarctic circumpolar current in Drake Passage. Oceanography 25(3):134–135. https://doi.org/10.5670/oceanog.2012.86
Donohue KA, Tracey KL, Watts DR, Chidichimo MP, Chereskin TK (2016) Mean Antarctic circumpolar current transport measured in Drake Passage. Geophys Res Lett. https://doi.org/10.1002/2016gl070319
Dufour CO, Griffies SM, de Souza GF, Frenger I, Morrison AK, Palter JB et al (2015) Role of mesoscale eddies in cross-frontal transport of heat and biogeochemical tracers in the Southern Ocean. J Phys Oceanogr 45(12):3057–3081. https://doi.org/10.1175/JPO-D-14-0240.1
Firing YL, Chereskin TK, Watts DR, Matthew MR (2016) Bottompressure torque and the vorticity balance from observations in Drake Passage. Journal of Geophysical Research: Oceans 121:4282–4302. https://doi.org/10.1002/2016JC011682
Fu L-L, Chelton D, Le Traon P-Y, Morrow R (2010) Eddy dynamics from satellite altimetry. Oceanography 23(4):14–25. https://doi.org/10.5670/oceanog.2010.02
Gille ST (1999) Evaluating southern ocean response to wind forcing. Phys Chem Earth Part A 24(4):423–428. https://doi.org/10.1016/S1464-1895(99)00053-8
Hughes CW, Meredith MP, Heywood KJ (1999) Wind-driven transport fluctuations through drake passage: a Southern Mode. J Phys Oceanogr 29(8):1971–1992. https://doi.org/10.1175/1520-0485(1999)029%3c1971:WDTFTD%3e2.0.CO;2
Kim YS, Orsi AH (2014) On the variability of antarctic circumpolar current fronts inferred from 1992–2011 altimetry*. J Phys Oceanogr 44(12):3054–3071. https://doi.org/10.1175/jpo-d-13-0217.1
Kleinherenbrink M, Riva R, Sun Y (2016) Sub-basin-scale sea level budgets from satellite altimetry, Argo floats and satellite gravimetry: a case study in the North Atlantic Ocean. Ocean Sci 12(6):1179–1203. https://doi.org/10.5194/os-12-1179-2016
Koelling J, Send U, Lankhorst M (2020) Decadal strengthening of interior flow of north atlantic deep water observed by GRACE satellites. J Geophys Res Oceans. https://doi.org/10.1029/2020jc016217
Leuliette EW, Miller L (2009) Closing the sea level rise budget with altimetry, Argo, and GRACE. Geophys Res Lett. https://doi.org/10.1029/2008gl036010
Liau JR, Chao BF (2017) Variation of Antarctic circumpolar current and its intensification in relation to the southern annular mode detected in the time-variable gravity signals by GRACE satellite. Earth Planets Space 69:1–9. https://doi.org/10.1186/s40623-017-0678-3
Makowski JK, Chambers DP, Bonin JA (2015) Using ocean bottom pressure from the gravity recovery and climate experiment (GRACE) to estimate transport variability in the southern Indian Ocean. J Geophys Res Oceans 120(6):4245–4259. https://doi.org/10.1002/2014jc010575
Mazloff MR, Boening C (2016) Rapid variability of Antarctic bottom water transport into the Pacific Ocean inferred from GRACE. Geophys Res Lett 43(8):3822–3829. https://doi.org/10.1002/2016gl068474
Meredith MP, Woodworth PL, Hughes CW, Stepanov V (2004) Changes in the ocean transport through Drake Passage during the 1980s and 1990s, forced by changes in the Southern Annular Mode. Geophys Res Lett. https://doi.org/10.1029/2004GL021169
Meredith MP, Woodworth PL, Chereskin TK, Marshall DP, Allison LC, Bigg GR et al (2011) Sustained monitoring of the southern ocean at drake passage: past achievements and future priorities. Rev Geophys. https://doi.org/10.1029/2010rg000348
Park J-H, Watts DR, Donohue KA, Jayne SR (2008) A comparison of in situ bottom pressure array measurements with GRACE estimates in the Kuroshio Extension. Geophys Res Lett. https://doi.org/10.1029/2008gl034778
Qin J, Cheng X, Yang C, Ou N, Xiong X (2022) Mechanism of interannual variability of ocean bottom pressure in the South Pacific. Clim Dyn. https://doi.org/10.1007/s00382-022-06198-0
Quinn KJ, Ponte RM (2011) Estimating high frequency ocean bottom pressure variability. Geophys Res Lett. https://doi.org/10.1029/2010gl046537
Rashid HA, Hendon HH, Wheeler MC, Alves O (2010) Prediction of the Madden–Julian oscillation with the POAMA dynamical prediction system. Clim Dyn 36(3–4):649–661. https://doi.org/10.1007/s00382-010-0754-x
Rintoul SR (2018) The global influence of localized dynamics in the Southern Ocean. Nature 558(7709):209–218. https://doi.org/10.1038/s41586-018-0182-3
Rintoul SR, Sokolov S (2001) Baroclinic transport variability of the Antarctic Circumpolar Current south of Australia (WOCE repeat section SR3). J Geophys Res Oceans 106(C2):2815–2832. https://doi.org/10.1029/2000jc900107
Sokolov S, Rintoul SR (2007) Multiple jets of the Antarctic circumpolar current South of Australia. J Phys Oceanogr 37(5):1394–1412. https://doi.org/10.1175/jpo3111.1
Tapley BD, Bettadpur S, Ries JC, Thompson PF, Watkins MM (2004) GRACE measurements of mass variability in the Earth system. Science 305(5683):503–505. https://doi.org/10.1126/science.1099192
Thompson AF, Sallee JB (2012) Jets and topography: jet transitions and the impact on transport in the Antarctic circumpolar current. J Phys Oceanogr 42(6):956–972. https://doi.org/10.1175/JPO-D-11-0135.1
Wang J, Wang J, Cheng XH (2015) Mass-induced sea level variations in the Gulf of Carpentaria. J Oceanogr 71(4):449–461. https://doi.org/10.1007/s10872-015-0304-6
Wang X, Zheng H, Zhu X-H, Zhao R, Wang M, Chen J et al (2023) Validation and evaluation of GRACE-FO estimates with in situ bottom pressure array measurements in the South China Sea. Remote Sensing. https://doi.org/10.3390/rs15112804
Watkins MM, Wiese DN, Yuan D-N, Boening C, Landerer FW (2015) Improved methods for observing Earth's time variable mass distribution with GRACE using spherical cap mascons. J Geophys Res Solid Earth 120(4):2648–2671. https://doi.org/10.1002/2014jb011547
Whitworth T, Nowlin WD, Worley SJ (1982) The net transport of the antarctic circumpolar current through Drake Passage. J Phys Oceanogr 12(9):960–971. https://doi.org/10.1175/1520-0485(1982)012%3c0960:TNTOTA%3e2.0.CO;2
Xu X, Chassignet EP, Firing YL, Donohue K (2020) Antarctic circumpolar current transport through Drake Passage: what can we learn from comparing high-resolution model results to observations? J Geophys Res Oceans. https://doi.org/10.1029/2020jc016365
Zhu Y, Yao J, Xu T, Li S, Wang Y, Wei Z (2022) Weakening trend of luzon strait overflow transport in the past two decades. Geophys Res Lett. https://doi.org/10.1029/2021GL097395

Publisher's Note

Springer Nature remains neutral with regard to jurisdictional claims in published maps and institutional affiliations.

Submit your manuscript to a SpringerOpen journal and benefit from:

- Convenient online submission
- Rigorous peer review
- Open access: articles freely available online
- High visibility within the field
- Retaining the copyright to your article

Submit your next manuscript at ► springeropen.com